Photoneutron Production with the Laser-Compton Backscattered Photons

Hiroyuki TOYOKAWA, Hideaki OHGAKI, Suguru SUGIYAMA, Tomohisa MIKADO, Kawakatsu YAMADA, Ryoichi SUZUKI, Toshiyuki OHDAIRA, Norihiro SEI, and Mitsukuni CHIWAKI

Electrotechnical Laboratory, IBARAKI 305-8568, Japan

A method to produce quasi-monoenergetic photoneutrons for detector calibration was examined. The photoneutrons were produced with a photo-induced neutron emission of a ^{9}Be using the Laser-Compton backscattered photons. Because the photon energy is continuously tunable, neutrons with various energies are obtained. Yield of the neutrons was measured with a liquid scintillation detector at the photon energies from 1651 keV to 3019 keV. Neutron yield at around the threshold energy for the $^{9}Be(\gamma,n)$ reaction was measured by changing the photon energy in a 10 keV step.

1. Introduction

Influences on human body of the exposure of the intermediate-energy neutrons with the energies from epithermal to about a few tens of keV play an important role on the evaluation of total dose. While monoenergetic neutron sources of intermediate energy are useful to calibrate neutron detectors, there are few neutron sources with these energies. A thin metal foil, such as scandium and beryllium, bombarded by an accelerated proton beam produces neutrons of a few tens of keV. However, the proton energy must be strictly controlled and a fluctuation of the energy deposition on a target should be small enough so that the neutron energy do not fluctuates.

Photoneutron sources using gamma-rays from radioisotopes produce monoenergetic neutrons with almost no energy fluctuation. Some photoneutron sources, such as ^{124}Sb-^{9}Be, ^{24}Na-^{9}Be, and ^{24}Na-D, are practically used as intermediate-energy neutron sources. Photoneutrons usually accompany with a large background of gamma-rays. Because the cross section for (γ,n) reaction is small, typically on the order of microbarns to millibarns, the ratio of the photoneutrons to gamma-rays from a typical photoneutron source is on the order of 10^{-5} to 10^{-6}. Moreover, the gamma-ray background is enhanced by the geometry of the photoneutron sources, because most of the photoneutron sources consists of a gamma-ray emitter surrounded by a photon-neutron converter and, hence, the neutrons and the gamma-rays are emitted into the same direction. Then, the neutrons will appear in a shower of background gamma-rays. Neutron separation energies for most nuclei are almost 8 MeV, except for ^{9}Be and ^{2}H (1666 keV and 2226 keV, respectively). So only these two materials are used as a photon-neutron converter. The gamma-ray energies from radioisotopes practically used as a photon-emitter are usually below about 3 MeV, because the life-time of the radioisotopes becomes too short as the gamma-ray energy became higher.

Although the photoneutron sources have a stability for the energy fluctuation, low neutron yield, high gamma-ray background, and the short life-time limit the use of the photoneutron sources. So, we have been trying to develop an energy-variable photoneutron source using the laser-Compton backscattered (LCS) photons [1].

2. LCS Photon Facility

The LCS photon facility of Electrotechnical Laboratory (ETL-LCS) [2] started its operation in 1984. It generates photon beams with the energies continuously tunable from 1 MeV to 40 MeV with an intensity of about 10^7 cm^{-2} s^{-1}. Figure 1 shows the layout of the ETL-LCS facility. LCS photons are produced with the Compton scattering of an intense beam of monochromatic photons, typically a laser beam, from relativistic electrons. In the ETL-LCS facility, an 800 MeV electron storage ring TERAS [3] is used as an electron source. Because most of the photons are backscattered (180°), the LCS photons are usually confined in a small solid angle at around a direction of the electron beam. Quasi-monochromatic photon beams are obtained by a collimation of the backscattered photons with an appropriate collimator. The solid angle subtended by the collimator at the laser-electron scattering point is usually on the order of 10^{-9} steradians.

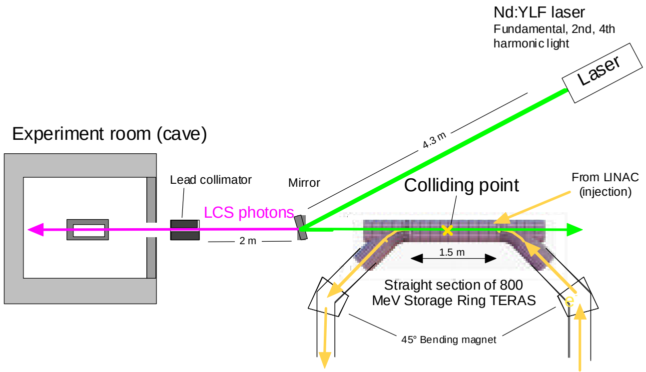

Fig. 1 Layout of the ETL-LCS facility.

3. Experiment

Figure 2 shows an experimental setup for the photoneutron measurement. We used a Q-switched Nd:YLF laser (1053 nm) whose repetition frequency and a pulse width were 5 kHz and 150 ns, respectively. The LCS photons that are collimated with a lead collimator of ϕ2 mm are incident on the front face of a ^{9}Be rod target (ϕ5 x 100 mm). Because the LCS photons are narrowly collimated, the target should be long, and as slender as possible to suppress an energy-degradation due to a scattering and absorption within the target. Then, it is placed along the axis of a cylindrical 4π neutron detector [4], which is filled with a gadolinium-loaded liquid scintillator (NE323).

The capture cross section of thermal neutrons of ^{155}Gd and ^{157}Gd is extremely large (6 x 10^4 and 2.5 x 10^5 barns, respectively). Some of the photoneutrons emitted from the target rod are captured by the gadolinium nuclei in the liquid scintillator. The gadolinium nuclei, then, emitt intense flashes of cascade gamma-rays which amounts to about 8 MeV per a captured neutron. The gamma-ray bursts tell the neutron detection as an intense flash of scintillation lights. Although the method is commonly used as a neutron counting [5], it is effective only for a large-tank detector when the cascade gamma-rays are fully absorbed. The size of our detector is, however, too small for the gamma-rays deposit all their energy into the detector. So, the flash was not distinguished simply with a pulse-height discrimination. We tried a pulse-shape discrimination, as well. Although the method itself was successful using an Am-Be neutron source, the neutron

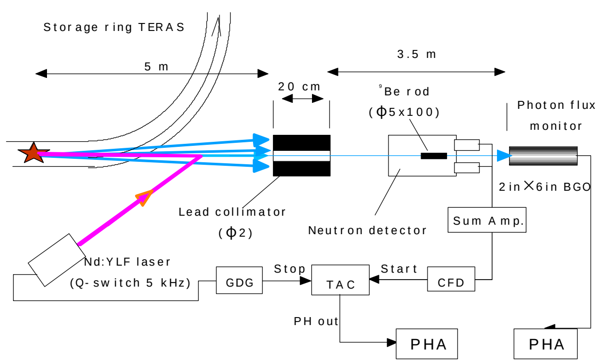

Fig. 2 Experimental setup for the photoneutron measurement.

signals were not distinguished from those of gamma-rays for the present experiment using the LCS photons, because of the signal pile-up of the neutrons and the gamma-rays. The LCS photons are generated in every 200 μs with the pulse width of 150 ns, so the photoneutrons are generated and enter the detector almost the same time as the annihilation and Compton-scattered photons from the target. Then, most of the signals will pile up.

Then, we tried to count neutrons with a time profile of a scintillation output. Neutrons are moderated in the detector, and some of them are captured. If the scintillation lights by recoil protons were discriminated by a pulse-height discrimination, only the gamma-ray signals are obtained. So, the neutron events are distinguished from the other signals with the time profile of the gamma-ray flashes, because they occur according to the neutron moderation, while the other events occur almost simultaneously as the photon incidence.

The block diagram of the signal processing system is shown in fig. 2. Signals from the photomultipliers summed by the sum-amplifier (Sum Amp.) were fed to the constant fraction discriminator (CFD), whose output is fed to the time-to-amplitude converter (TAC) as a start signal. A trigger signal from the laser, properly delayed with the gate-and-delay generator (GDG), stop the time-to-amplitude conversion. The pulse height from the TAC is analyzed with a multichannel analyzer.

Photon flux is monitored with a BGO detector placed at the back of the target rod. Attenuation of the flux was evaluated by experiments using a blank target. The flux is reduced to about half of the incident photons at 1700 keV. The energy of the LCS photons was tuned by changing the electron energy of the storage ring according to the following formula:

$$E_{\gamma\,\max} = \frac{4E_e^{\,2}\varepsilon_L}{m_0c^2 + 4E_e\varepsilon_L}$$

Where $E_{\gamma_{max}}$, E_e, ε_L are the maximum photon energy, electron energy, and the energy of the laser photon quanta, respectively, and m_0c^2 is the electron rest mass. Figure 3 shows a pulse height spectrum for the 2975 keV LCS photons measured with a HPGe of 120 % relative efficiency. The energies of the LCS photons were measured with the HPGe detector during the experiments. Maximum and mean energies of the LCS photons used in the present experiments are summarized in table 1.

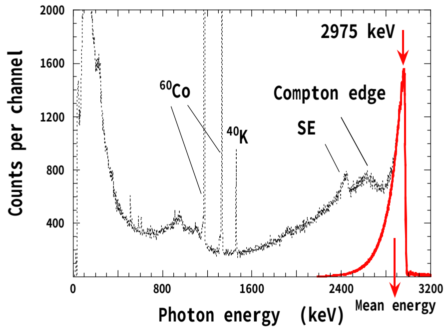

Fig. 3 Pulse height spectrum from a HPGe of 120 % relative efficiency for the 2975 keV photons (broken line). A sharp spike (thick solid line) corresponds to the LCS photons. A mean energy is 2879 keV.

4. Discussion

Figure 4 shows the time profiles of the gamma-ray flashes, which were measured below (1651 keV) and above (1707 keV) the threshold energy for the ^{9}Be(γ,n) reaction. A sharp spike in the figure is due to the annihilation or the Compton-scattered photons from the target caused by the LCS photons, and, hence, it indicates the incident time of the LCS photons. The prompt photon emission extended about 3 μs after the photon incidence. The bump, peaked at about 8 μs after the incidence of the LCS photons are due to the neutrons from the target, and only seen in the time profile measured above the threshold energy. It was necessary to keep the count rate of the prompt flashes low enough to prevent the neutron-induced flashes merge into the prompt flashes, because the neutron gamma-ray event ratio in the present experiments was 10^{-4} to 10^{-5}, which is summarized in table 1. So, the count rates for the prompt flashes were kept less than 50 cps during the experiment by a proper attenuation of the LCS photons with lead plates.

While the absolute yield of the photoneutrons can not be deduced, because the detection efficiency of the neutron detector is currently unknown, relative yield and the (γ,n) cross section times the detection efficiency were measured and summarized in table 1. Figure 5 shows the (γ,n) cross section assuming the constant detection efficiency of 15 %, which was deduced by fitting the present data to that of Berman et al. [5], at 1670 keV. The present data showed a sharp rise at 1666 keV, and the maximum value was seen at about 10 keV above.

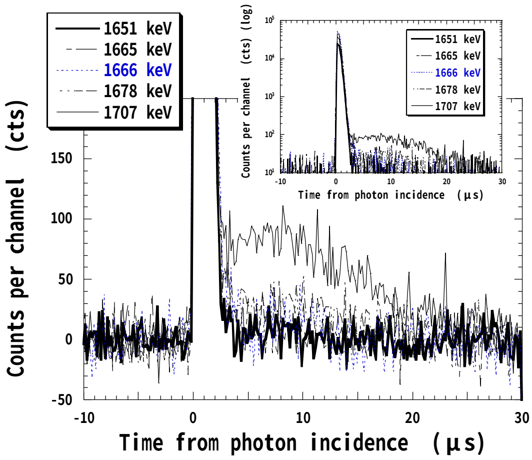

Fig. 4 Time profiles of the gamma-ray flashes. The maximum photon energies are indicated in the figure. The small figure at right-hand is the whole view of the spectra (log).

Table 1 Experimental results of the photoneutron experiment. E_{max} and E_{ave} are the maximum and mean energy of the LCS photons. Neutron yield per gamma-ray and the uncertainty are summarized in column 3, the measured value of the(γ,n) cross sections are listed together with the uncertainty in column 4. Cross section assuming the detection efficiency of 15 % is listed in column 5.

E_{max} (keV)	E_{ave} (keV)	n-γ ratio (× 10^{-5})	ε*σ (10^{-29} barn)	σ (mb)
1650.6	1650.6	NA	NA	NA
1664.9	1664.9	NA	NA	NA
1666.4	1666.0	14.2 ± 4.2	11.2 ± 3.3	0.747 ± 0.220
1678.3	1670.6	30.0 ± 3.6	23.7 ± 2.8	1.580 ± 0.187
1707.0	1685.3	20.1 ± 2.5	15.9 ± 2.0	1.060 ± 0.133
2080.0	1888.5	5.61 ± 0.58	4.43 ± 0.46	0.295 ± 0.031
2145.8	1948.2	4.35 ± 0.45	3.43 ± 0.36	0.229 ± 0.024
2200.0	1997.4	3.70 ± 0.39	2.92 ± 0.31	0.195 ± 0.021
2934.7	2840.2	8.02 ± 0.84	6.33 ± 0.65	0.422 ± 0.043
2954.3	2859.2	8.09 ± 0.84	6.39 ± 0.66	0.426 ± 0.044
2964.6	2869.1	8.80 ± 0.91	6.95 ± 0.72	0.439 ± 0.048
2974.8	2878.9	9.44 ± 0.97	7.45 ± 0.77	0.497 ± 0.051
2990.2	2893.9	9.93 ± 1.0	7.84 ± 0.81	0.523 ± 0.054
2999.5	2902.9	10.7 ± 1.1	8.45 ± 0.87	0.563 ± 0.058
3010.8	2913.9	11.1 ± 1.1	8.76 ± 0.91	0.584 ± 0.061
3019.0	2921.8	15.8 ± 1.6	1.25 ± 0.13	0.833 ± 0.087

6. Conclusion

Photoneutron yield of a ^{9}Be rod was measured by using the Laser-Compton backscattered photons. The neutrons were counted with the Gd-loaded liquid scintillator. The prompt flash was seen within 3 μs of the photon incidence, and the delayed one followed, which was peaked at about 8 μs. The former flashes are due to the annihilation and the Compton-scattered photons from the target, while the latter corresponds to the gamma-ray cascade from gadolinium nuclei due to the neutron capture. Relative yield of the photoneutrons and the ^{9}Be(γ,n) cross section folded by the detection efficiency of the neutron detector were measured in the energy range from 1650 keV to 3019 keV, while the absolute cross section was not obtained, yet. If the detection efficiency of the neutron detector was calibrated, the absolute value will be obtained. A Monte Carlo simulation will be helpful for a measurement of the response function of the neutron detector.

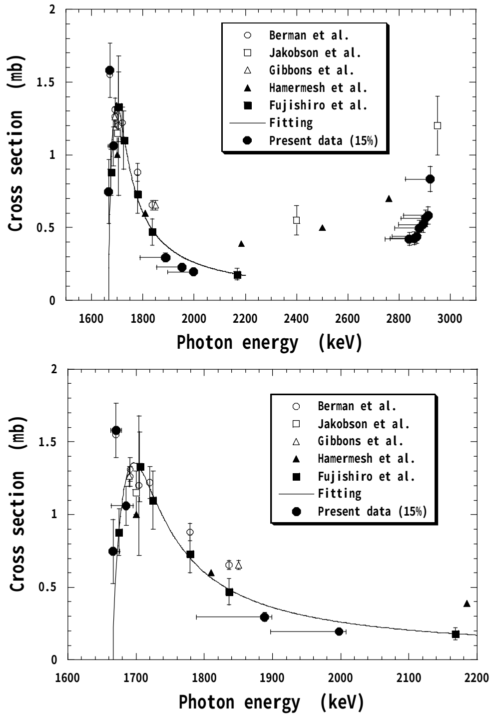

Fig. 5 (γ,n) cross sections measured in the present experiment (black circles) in the energy range from 1500 keV to 3000 keV (above), and from 1600 keV to 2200 keV (below). Reference data are those of Berman et al. [6] (open circles), Jakobson [7] (squares), Gibbons et al. [8] (triangles), Hamermesh et al. [9] (black triangles), Fujishiro et al. [10] (black squares). The fitting curve (solid line) was taken from ref. 9.

Acknowledgements

We would like to thank Professor Hiroaki Utsunomiya of Konan University for valuable discussions. This work was supported by Science and Technology Agency of Japan.

References

[1] R.H. Milburn: Phys.Rev. Lett. **10**(1963)75.
[2] T. Yamazaki et al.: IEEE Trans. Nucl. Sci. **32**[5](1985)3406..
[3] T. Tomimasu et al.: IEEE Trans. Nucl. Sci., **30**[4](1983)3133
[4] H. Toyokawa et al.: Nucl Instr. and Meth. **A422**(1999)95.
[5] H. Beil, R. Bergere and A. Veyssiere: Nucl. Instr. And Meth. **67**(1969)293.
[6] B. L. Berman, R. L. Van Hemert, and C. D. Bowman: Phys. Rev. 163[4](1967)163.
[7] Mark J. Jakobson: Phys. Rev. **123**[1](1961)229.
[8] J. H. Gibbons, R. L. Macklin, J. B. Marion, and H. W. Schmitt,: Phys. Rev. **114**[5](1959)1319
[9] B. Hamermesh and C. Kimball: Phys. Rev. **90**[6](1953)1063.
[10] M. Fujishiro, T. Tabata, K. Okamoto, and T. Tsujimoto: Can. J. Phys. **60**(1982)1672.